Robust OFDM Receivers for Dispersive Time-Varying Channels: Equalization and Channel Acquisition

Alexei Gorokhov, *Associate Member, IEEE,* and Jean-Paul Linnartz, *Senior Member, IEEE*

***Abstract*—In orthogonal frequency-division multiplexing, time variations of a multipath channel lead to a loss of orthogonality between the subcarriers, and thereby limit the achievable throughput. This paper proposes a general framework for a controlled removal of intercarrier interference (ICI) and channel acquisition. The core idea behind our method is to use a finite power series expansion for the time-varying frequency response, along with the known statistical properties of mobile radio channels. Channel acquisition and ICI removal are accomplished in the frequency domain and allow for any desired tradeoff between the residual ICI level, the required training for channel acquisition, and processing complexity. The proposed approach enables a high spectral efficiency (64-quadrature amplitude modulation mode) of digital video broadcasting-terrestrial in highly mobile environments.**

***Index Terms*—Digital video broadcasting (DVB), intercarrier interference (ICI), mobile communications, multicarrier systems.**

I. Introduction

In ORTHOGONAL frequency-division multiplexing (OFDM), multiple user symbols are transmitted simultaneously over orthogonal subcarriers which form an OFDM symbol [1]–[6]. Compared to other modulation methods, OFDM symbols have a relatively long time duration, whereas each subcarrier has a narrow bandwidth. The bandwidth of each subcarrier is small enough to assume a flat (nonselective) fading in a moderately frequency-selective channel. These subcarriers have overlap in time and frequency domains, nonetheless, the signal waveforms are designed to be orthogonal, due to a cyclic extension of each OFDM symbol in the time domain. A practical implementation involves the inverse fast Fourier transform (IFFT) at the transmitter and the fast Fourier transform (FFT) at the receiver. The narrowband nature of subcarriers makes the signal robust against frequency selectivity caused by a multipath delay spread. However, OFDM is relatively sensitive to its dual, namely, time selectivity, which is due to rapid time variations of a mobile channel. Time variations corrupt the orthogonality of the OFDM subcarrier waveforms so that intercarrier interference (ICI) occurs.

Paper approved by C. Tellambura, the Editor for Modulation and Signal Design of the IEEE Communications Society. Manuscript received June 24, 2002; revised August 5, 2003. This paper was presented in part at the IEEE International Conference on Communications, New York, NY, May 2002.

A. Gorokhov was with the Philips Research National Laboratory, 5656 AA Eindhoven, The Netherlands. He is now with Qualcomm Inc., San Diego, CA 92121 USA (e-mail: gorokhov@qualcomm.com).

J.-P. Linnartz is with the Philips Research National Laboratory, 5656 AA Eindhoven, The Netherlands (e-mail: j.p.linnartz@philips.com).

Digital Object Identifier 10.1109/TCOMM.2004.826354

In a stationary channel, OFDM requires only a straightforward signal processing to combat channel delay spreads. This was a prime motivation to use OFDM modulation methods in several standards, such as digital audio broadcasting (DAB), digital terrestrial television broadcasting (DTTB/DVB-T), and more recently, wireless LAN standards such as IEEE-802.11a and HIPERLAN/2. The main parameters of these systems have been selected to prevent a noticeable time selectivity from occuring in the foreseen range of propagation environments which do not account for high mobility. Nonetheless, one can notice an increasing demand for the use of DVB-T in mobile applications.

Both OFDM and multicarrier code-division multiple access (MC-CDMA) (a spread-spectrum version of the OFDM [7], [8]), are being considered as candidates for future generation mobile phone and multimedia communication standards. The separation into multiple subcarriers allows relatively high data rates. Studies such as the one reported in this paper show that OFDM transmission can be protected against time dispersion. This significantly extends the scope of admissible parameters, application areas, and design options for such future air interfaces.

The problem of robust OFDM reception in mobile environments has been addressed recently by several authors. The effect of channel variations for the ICI has been addressed in [9]. Statistical properties of ICI are discussed in [10] for some practically important cases. In [11], a statistical approach to channel estimation is presented which is based on the standard models of time-varying channels [12], [13]. A numerically efficient suboptimal channel estimator from [11] allows reducing the frequency of channel-acquisition phases and track channel parameters. Yet, relatively slow channel variations are assumed so that ICI is fully neglected. In [14], the standard statistical model is used to estimate the parameters of a time-varying channel via the expectation-maximization (EM) algorithm, thereby making use of the data symbols along with pilots and/or training. An attractive feature of this approach lies in a possibility to reduce the training overhead. However, the excessive complexity of EM iterations makes an implementation hardly possible, even for a moderate number of channel parameters. The authors of [15] propose to modulate a few subcarriers by the same data symbol, via the so-called polynomial cancellation coding. A similar idea has been presented in [16]. Although this method yields a valuable performance gain (around 15 dB for every extra subcarrier per symbol), it implies a substantial reduction in spectral efficiency. Also, this technique is not applicable to the existing systems.

Recently, a new equalization technique has been proposed in [17] and [18]. The main results are due to an observation that

time variations of a channel response may be assumed linear over an OFDM block, for moderate Doppler spreads. This observation led the authors to a simplified ICI model introduced in [17].

The data model from [17] appears to be a particular case of a more general statistical model developed in this paper. As explained in Section II, the core idea behind our model is to make use of stochastic power series expansion of the time-varying terms which are owing to Doppler offsets of individual scatterers. A finite power series expansion gives rise to a compact parameterization of time-varying channels with a closed-form statistical characterization given in Section III. The data and channel model are used to design channel estimation procedures in Section IV-A. We propose some simplifications of the optimal training-based estimator, due to the covariance structure of a time-varying channel and some asymptotic properties for big block sizes. Sections V and VI discuss linear minimum mean-square error (LMMSE) and decision-feedback equalization (DFE) and leakage removal, respectively. Once again, particular attention is paid to reduction of the implementation complexity which is achieved due to the structural properties of the data model. A numerical analysis of the approach described in this paper is addressed in Section IX. We focus on a DVB application with the European DVB-T standard being considered as a reference system. Its' 2-K and 8-K transmission modes specify 2048 and 8192 subcarriers, respectively, with the total bandwidth of 6–8 MHz. The substantial ICI that arises in mobile environments (with a terminal velocity of 100 km/h and more) significantly affects the system performance in the high spectral efficiency mode, i.e., when quadrature amplitude modulation (QAM)-64 is used. Our numerical study suggests that the quality of service (QoS) requirements can be met due to our approach.

II. Mobile Multipath Channel in Frequency Domain

In this section, we derive a finite-order model that captures statistical properties of the frequency channel response and ICI of a mobile multipath channel. This model will be used throughout this paper.

A. Channel Parameters

Consider a linear multipath propagation channel characterized by a possibly infinite set of specular paths with the respective complex amplitudes $\{h_l\}$, delays $\{\tau_l\}$, and angles of arrival $\{\theta_l\}$. We make use of the standard assumption that the mobile channel consists of uncorrelated Rayleigh paths with a uniform angle distribution and exponentially decaying delay profile defined by a root mean square (rms) delay spread τ_0

$$\sum_{\substack{\theta_l\in(\theta,\theta+d\theta)\\ \tau_l\in(\tau,\tau+d\tau)}} \mathbb{E}\left\{|h_l|^2\right\} = \frac{1}{2\pi\tau_0}\exp\left(-\frac{\tau}{\tau_0}\right)d\tau d\theta \qquad (1)$$

$\theta \in (-\pi,\pi)$, $\tau \geq 0$, where $\mathbb{E}\{\cdot\}$ stands for the expectation. We also assume that the mobile station has a certain velocity, giving rise to a maximum Doppler shift f_d for paths arriving at zero angle of incidence so that the Doppler shift of the lth path is $f_l = f_d\cos\theta_l$. These assumptions are commonly used to describe mobile radio channels, see, e.g., [12], [13], and [19].

B. OFDM Signal With ICI

Consider the conventional OFDM system, where each data is a sum of N orthogonal subcarriers, each with a rectangular envelope. The subcarriers are modulated by N data symbols by means of the N-point IFFT. Each block of N samples is extended with a cyclic prefix and transmitted after an appropriate pulse shaping. Denote $\boldsymbol{s} = [\boldsymbol{s}_0,\ldots,\boldsymbol{s}_{N-1}]^T$ the vector of data symbols (here $[\cdot]^T$ denotes matrix transpose) and $g_r(t)$, the time response of a square-root Nyquist filter. The transmitted baseband signal may be written as follows:

$$s(t) = \frac{1}{\sqrt{N}}\sum_{k=0}^{N-1}\sum_{i=0}^{N+L-1}\boldsymbol{s}_k e^{\frac{\imath 2\pi k(i-L)}{N}} g_r(t-iT) \qquad (2)$$

$t\in(0,(N+L)T)$, where T is the data sample period, L is the length of the cyclic extension (prefix), and $\imath=\sqrt{-1}$. Later in this paper, the data symbols $\boldsymbol{s}$ are assumed zero mean and unit variance independent identically distributed (i.i.d.). The transmitted signal undergoes a time-varying multipath channel described in the previous paragraph. The received noisy signal verifies

$$x(t) = \sqrt{E_s}\sum_l h_l s(t-\tau_l)e^{\imath 2\pi f_l t} + n(t) \qquad (3)$$

where E_s is signal energy per channel use and $n(t)$ is additive white Gaussian noise (AWGN) within the signal bandwidth, with the variance $(N_0/2)$ per complex dimension. We additionally assume that Doppler spread is much smaller than the signal bandwidth. The output of the receiver filter matched to $g_r(t)$ yields

$$\tilde{x}(t) = \sqrt{\frac{Es}{N}}\sum_l\sum_{k=0}^{N-1}\sum_{i=0}^{N+L-1}\boldsymbol{s}_k e^{\frac{\imath 2\pi k(i-L)}{N}} \cdot h_l g(t-\tau_l-iT)e^{\imath 2\pi f_l t} + \tilde{n}(t) \qquad (4)$$

where $g(t)$ is the time response of the Nyquist filter and $\tilde{n}(t)$ is the filtered noise. The matched-filter output is sampled at rate $(1/T)$ at a certain time offset t_0. Finally, the N-point FFT is applied to a set of N samples $\{\tilde{x}(t_0+jT)\}_{0\leq j<N}$ with a reconstruction delay (δT), resulting in a vector $\boldsymbol{y} = [\boldsymbol{y}_0,\ldots,\boldsymbol{y}_{N-1}]^T$ so that

$$\begin{aligned}\boldsymbol{y}_m &= \frac{1}{\sqrt{N}}\sum_{j=0}^{N-1}\tilde{x}(t_0+jT)e^{\frac{-\imath 2\pi m(j-\delta)}{N}}\\ &= \frac{\sqrt{Es}}{N}\sum_{j=0}^{N-1}\sum_l\sum_{k=0}^{N-1}\sum_{i=0}^{N+L-1}\boldsymbol{s}_k e^{\frac{\imath 2\pi(k(i-L)-m(j-\delta))}{N}}\\ &\quad\cdot h_l g\left(t_0-\tau_l+(j-i)T\right)e^{\imath 2\pi f_l(t_0+jT)} + \boldsymbol{n}_m\end{aligned}$$

where $\boldsymbol{n} = [\boldsymbol{n}_0,\ldots,\boldsymbol{n}_{N-1}]^T$ are the noise samples after the FFT. The latter expression may be written as

$$\boldsymbol{y}_m = \sqrt{Es}\sum_{k=0}^{N-1}\boldsymbol{s}_k\frac{1}{N}\sum_{j=0}^{N-1}e^{\frac{-\imath 2\pi(m-k)(j-\delta)}{N}} \cdot\sum_l\tilde{H}_l[k]e^{\imath 2\pi f_l T(j-\delta)} + \boldsymbol{n}_m \qquad (5)$$

$$\tilde{H}_l[k] = h_l e^{\imath 2\pi f_l(t_0+\delta T)} e^{\frac{\imath 2\pi k(\delta - L)}{N}} \cdot \sum_p g(t_0 - \tau_l + pT) e^{\frac{-\imath 2\pi kp}{N}} \quad (6)$$

wherein the assumption is made that t_0 and L are chosen so that for any $0 \le j < N$ and τ_l within the significant part of the delay spread, the space $(t_0 - \tau_l + (j-i)T)$ covers the *effective* span of $g(t)$.

Note that the reconstruction delay is introduced inside the FFT, which is quite different from delaying the received signal. Alternatively, this delay may be interpreted/implemented as a cyclic delay (shift) of the sequence of N samples $\{\tilde{x}(t_0 + jT)\}_{0 \le j < N}$ prior to the FFT. Such a reconstruction delay gives us a freedom to set the reference time for the time-varying channel. It is convenient to choose (δT) in the middle of the examined time interval. Such a choice of the reference time implies minimum magnitude of time-varying channel fluctuations over the whole interval. Hence, we will consider $\delta = (N-1)/2$.

Whenever $f_d = 0$, we have $f_l = 0$ for all l, and therefore, (5) yields $\boldsymbol{y}_m = H_m \boldsymbol{s}_m + \boldsymbol{n}_m$, $H_m = \sum_l \tilde{H}_l[m]$. As expected, the effect of this static channel is limited to a pointwise multiplicative distortion of the subcarriers by the static channel frequency response $\{H_m\}_{0 \le m < N}$. Some ICI appears when $f_d \neq 0$, and is reflected by the fact that inner sum (with respect to (w.r.t.) l) in (5) depends on j when $f_l \neq 0$.

In this paper, we analyze the impact of Doppler spread on ICI via the power series expansion of the Doppler-driven terms $\exp(\imath 2\pi f_l T(j-\delta))$ w.r.t. $(f_l T)$ around $(f_l T = 0)$. The main advantage of such a representation comes from the fact that the Doppler spread remains relatively small in practical situations. In most cases, this series expansion will have a limited number of meaningful terms, giving rise to a limited number of parameters. Define the subcarrier spacing $f_s = 1/(TN)$ and the set of coefficients $H_k^{(p)}$

$$H_k^{(p)} = \frac{\left(\frac{\imath 2\pi f_d}{f_s}\right)^p}{p!} \sum_l \left(\frac{f_l}{f_d}\right)^p \tilde{H}_l[k], \quad 0 \le k < N \quad (7)$$

where $p \ge 0$. Due to the power series expansion $e^{\imath 2\pi f_l T j} = \sum_{p \ge 0} (\imath 2\pi f_l T j)^p / p!$, we may rewrite (5) as follows:

$$\boldsymbol{y}_m = \sqrt{Es} \sum_{p \ge 0} \sum_{k=0}^{N-1} \boldsymbol{s}_k H_k^{(p)} \Xi_{m,k}^{(p)} + \boldsymbol{n}_m$$
$$\Xi_{m,k}^{(p)} = \frac{1}{N} \sum_{j=0}^{N-1} \left(\frac{j-\delta}{N}\right)^p e^{\frac{-\imath 2\pi (m-k)(j-\delta)}{N}}. \quad (8)$$

The latter expression may be written in a closed-matrix form

$$\boldsymbol{y} = \sqrt{E_s} \left(\sum_{p \ge 0} \boldsymbol{\Xi}^{(p)} \mathrm{diag}\left\{ H^{(p)} \right\} \right) \boldsymbol{s} + \boldsymbol{n}$$
$$H^{(p)} = \left[H_0^{(p)}, \ldots, H_{N-1}^{(p)} \right]^T$$
$$\boldsymbol{\Xi}^{(p)} = \left\{ \Xi_{m,k}^{(p)} \right\}_{0 \le m,k < N}. \quad (9)$$

In the above expression, the off-diagonal entries of Toeplitz matrices $\boldsymbol{\Xi}^{(p)}$ specify the *fixed* magnitude of ICI. These matrices will be later addressed as *leakage* matrices. The channel-specific contribution is defined by the vectors $H^{(p)}, p = 0, 1, 2, \ldots$. To interpret these parameters, we note that $H_k^{(p)}$ defined in (7) equals, up to a scaling, the pth-order derivative of the sum

$$\sum_l \tilde{H}_l[k] e^{\imath 2\pi f_l T(j-\delta)} \quad (10)$$

w.r.t. the time variable (jT), which sum is the time-varying frequency response of the channel at the kth subcarrier. We will deliberately call $H_k^{(p)}$ the derivatives of the channel frequency response, or simply, *derivatives*. One can check that zeroth-order derivatives $H_k^{(0)}$ coincide with the static channel frequency response H_k. To distinguish between the parameters $\{H_k^{(0)}\}$ of the static component of the channel and the parameters $\{H_k^{(p)}\}$, $p > 0$ of its dynamic component, we will call the former ones the *amplitudes*. Note that the zeroth-order leakage matrix equals the identity matrix $\boldsymbol{\Xi}^{(0)} = \boldsymbol{I}_N$. It is easy to check that for $\delta = (N-1)/2$, the first-order leakage matrix $\boldsymbol{\Xi}^{(1)}$ satisfies

$$\Xi_{m,k}^{(1)} = \begin{cases} 0, & m = k \\ -N^{-1} \frac{e^{\frac{-\imath 2\pi(k-m)\delta}{N}}}{1 - e^{\frac{\imath 2\pi (k-m)}{N}}}, & m \neq k. \end{cases} \quad (11)$$

It is intuitively clear that for a slowly varying channel, only a limited set of p will have a significant contribution. We next study statistical properties of the derivatives.

III. Channel Statistics

In the following statistical analysis, we will assume that a multipath channel consists of a large number of statistically independent individual scatterers which continuously fill the propagation delay profile. This technical assumption is used to simplify the analysis, specifically to handle the indeterminacy of the sampling offset t_0. This assumption does not limit the scope of the main results reported in this paper.

As1: Elements of $\{h_l \exp(\tau_l/(2\tau_0))\}_{l=0,1,2,\ldots}$ are random circular zero-mean i.i.d. quantities, such that for any $\tau, d\tau > 0$, there exists $l : \tau_l \in (\tau, \tau + d\tau)$.

Let us now address the effect of the sampling offset t_0 and its effect for the channel parameters. The choice of t_0 becomes critical when the excess bandwidth is nonzero and the received data are sampled at the rate $(1/T)$. Sampling at the data rate leads to a loss in signal-to-noise ratio (SNR) at the receiver, and t_0 is chosen so as to maximize the SNR. Such a value of t_0 depends on the channel realization and, according to (6) and (7), so do $\{H_k^{(p)}\}$. The relationship between $\{H_k^{(p)}\}$ and $\{h_k, \tau_k\}$ is rather complicated, mainly due to a complex relationship between these latter and t_0. A closed-form result derived in this paper is due to **As1**. Indeed, the assumption of a "densely filled" impulse response with independent scatterers yields a *deterministic* timing t_0 which satisfies

$$t_0 = \arg\max_t \int_0^\infty e^{-\frac{\tau}{\tau_0}} \left| \sum_i g(t_0 - \tau + iT) e^{-\imath \frac{2\pi k i}{N}} \right|^2 d\tau$$

see the Appendix. Given a fixed timing t_0, we can compute the covariances of amplitudes and derivatives, according to (6) and (7). Due to **As1** and $(f_l/f_d) = \cos\theta_l$, we find

$$\mathbb{E}\left\{H_k^{(p)} H_{k'}^{(q)^*}\right\} = \frac{\left(\frac{\imath 2\pi f_d}{f_s}\right)^{p+q}}{(-1)^q p!q!} \cdot \sum_{l,i,i'} \mathbb{E}\left\{|h_l|^2 (\cos\theta_l)^{p+q} \times g(t_0 - \tau_l + iT) g(t_0 - \tau_l + i'T)\right\} \cdot e^{-\imath 2\pi \frac{ki - k'i'}{N}}$$

where $(^*)$ stands for the complex (Hermitian) conjugate and the expectation is w.r.t. the channel parameters $\{h_l\}$ and $\{\theta_l\}$ under the model (1). To compute this expectation, we make use of the result

$$\frac{1}{2\pi} \int_{-\pi}^{\pi} (\cos\theta)^{p+q} d\theta = \begin{cases} \frac{(p+q-1)!!}{(p+q)!!}, & \text{even } (p+q) \\ 0, & \text{odd } (p+q). \end{cases} \tag{12}$$

We also exploit the following standard property of a Nyquist filter:

$$\sum_i g(t_0 - \tau + iT) e^{\frac{-\imath 2\pi ki}{N}} = e^{\imath 2\pi f_s (t_0 - \tau) k} \tag{13}$$

where $0 \le k < N$. The results of (12) and (13) lead to

$$\begin{aligned} \mathbb{E}\left\{H_k^{(p)} H_{k'}^{(q)^*}\right\} &= \frac{(-1)^{\frac{p-q}{2}}}{p!q!} \frac{(p+q-1)!!}{(p+q)!!} \left(\frac{2\pi f_d}{f_s}\right)^{p+q} \\ &\quad \cdot \frac{1}{\tau_0} \int_0^{\infty} \exp\left(\frac{-\tau}{\tau_0}\right) e^{\imath 2\pi f_s (t_0 - \tau)(k - k')} d\tau \\ &= \frac{(-1)^{\frac{p-q}{2}}}{p!q!} \frac{(p+q-1)!!}{(p+q)!!} \\ &\quad \times \frac{\left(\frac{2\pi f_d}{f_s}\right)^{p+q}}{1 + \imath 2\pi f_s \tau_0 (k - k')} e^{\imath 2\pi f_s t_0 (k - k')} \end{aligned}$$

for even $(p+q)$, and 0, otherwise. Let us make two observations. First of all, the effect of the timing t_0 for channel correlations is equivalent to the effect of a delay for the channel frequency response. This effect may be removed completely, e.g., via multiplying the signal of the kth subcarrier by $\exp(-\imath 2\pi f_s t_0 k)$ upon the timing recovery. Therefore, we assume $t_0 = 0$ for the rest of this paper. Second, we notice that the terms containing (k, k') are decoupled from those with (p, q), i.e., the indexes (k, k') and (p, q) appear in two different multiplicative terms in the expression for $\mathbb{E}\{H_k^{(p)} H_{k'}^{(q)^*}\}$. Denote P the order of channel approximation and a $(P+1)N \times 1$ vector $H = [H^{(0)^T}, \ldots, H^{(P)^T}]^T$. Then the covariance matrix of H, $\boldsymbol{R} = \mathbb{E}\{HH^*\}$, satisfies

$$\boldsymbol{R} = \boldsymbol{R}_c \otimes \boldsymbol{R}_f \tag{14}$$

$$[\boldsymbol{R}_f]_{k,k'} = (1 + \imath 2\pi f_s \tau_0 (k - k'))^{-1} \tag{15}$$

$$[\boldsymbol{R}_c]_{p,q} = \begin{cases} \frac{(-1)^{\frac{p-q}{2}}}{p!q!} \frac{(p+q-1)!!}{(p+q)!!} \left(\frac{2\pi f_d}{f_s}\right)^{p+q}, & \text{even } (p+q) \\ 0, & \text{odd } (p+q) \end{cases} \tag{16}$$

where $(\otimes)$ stands for the Kronecker product, $\boldsymbol{R}_c$ is the $(P+1) \times (P+1)$ *coupling matrix* which consists of correlations between the derivatives of different orders, and $\boldsymbol{R}_f$ is the $N \times N$ *channel correlation matrix* containing correlations of the frequency response. Finally, we note that **As1**, along with the central limit theorem, imply that H is zero-mean circular Gaussian

$$H \sim \mathcal{N}_c(0, \boldsymbol{R}). \tag{17}$$

The proposed description of a time-varying channel frequency response may be seen as a two-dimensional (2-D) parameterization, wherein the two decoupled dimensions represent frequency domain correlations on one hand, and correlations between the derivatives on the other hand. This model differs from the standard 2-D model (see, e.g., [11]) in that the time dimension, commonly used to represent time variations of the frequency response, is replaced here by the dimension of time-invariant derivatives of the frequency response. For slow and moderate time variations, a small number of derivatives will accurately model the channel frequency response, resulting in a compact parameterization. As it follows from (15), the power of the pth derivative decays as the $2p$th power of the ratio between the Doppler spread f_d and the subcarrier spacing f_s. This ratio remains a small fraction of one in practice.

The described channel model relies on $N(P+1)$ parameters of the vector H to be estimated. This number is still too big for the block size N of practical interest. However, the effective number of degrees of freedom appears to be much smaller whenever the propagation delay spread τ_0 is a fraction of the OFDM block size NT. This fact is reflected by the structure of $\boldsymbol{R}_f$. Due to the asymptotic isomorphism property of Toeplitz–Hermitian matrices [20], the ordered eigenvalues of $\boldsymbol{R}_f$ converge to N times the sequence of its generating power spectrum sampled at fractions (k/N) of the unit circle, $0 \le k < N$, as $N \to \infty$. According to (15), the eigenspectrum of $\boldsymbol{R}_f$ converges to the sequence $\{((1 - \exp(-(f_s\tau_0)^{-1}))(f_s\tau_0))^{-1} \exp(-kT/\tau_0)\}_{0 \le k < N}$ as N grows. Such an exponential decay with a limited ratio (τ_0/T) allows for an accurate approximation of $\boldsymbol{R}_f$ with a finite number of its principal components. Let us define $\underline{U}$ a semiunitary $N \times \underline{N}$ matrix of eigenvectors corresponding to the $\underline{N}$ principal components of $\boldsymbol{R}_f$, a $\underline{N} \times \underline{N}$ diagonal matrix $\underline{\boldsymbol{R}}_f = \underline{U}^* \boldsymbol{R}_f \underline{U}$ of eigenvalues and $\underline{H} = \underline{U}^* H$. We have

$$H = (\boldsymbol{I}_{P+1} \otimes \underline{U}) \underline{H}, \quad \underline{H} \sim \mathcal{N}_c(0, \boldsymbol{R}_c \otimes \underline{\boldsymbol{R}}_f) \tag{18}$$

where $\underline{N} > f_s\tau_0$, and therefore, the number of model parameters reduces to $\underline{N}(P+1)$.

IV. Channel Response Estimation

The estimation algorithms described in this section make use of reference signals. Such reference signals are available during the training phase. Note that the detected data symbols, upon successful demodulation of a data block, may be reused as a reference signal to track the channel.

First of all, we derive a statistically optimal estimation procedure that relies upon the data model (9), and a reduced-complexity statistical channel model summarized in (18). We will show that the optimal approach leads to a simple suboptimal solution.

A. Maximum-Likelihood Estimator

Assume that a reference OFDM block $\underline{\boldsymbol{s}}$ is used to estimate the channel. Let $\underline{\boldsymbol{y}}$ and $\underline{\boldsymbol{n}}$ be the corresponding received signal and noise in the frequency domain. According to (9)

$$\underline{\boldsymbol{y}} = \sqrt{E_s}\left(\sum_{p\geq 0}\boldsymbol{\Xi}^{(p)}\mathrm{diag}\left\{H^{(p)}\right\}\right)\underline{\boldsymbol{s}} + \underline{\boldsymbol{n}}. \tag{19}$$

To concentrate on the reduced parameter set $\underline{H}$, we may rewrite (19), taking into account (18), as follows:

$$\begin{aligned}\underline{\boldsymbol{y}} &= \sqrt{E_s}\underline{\boldsymbol{\Xi}}\,\underline{H} + \underline{\boldsymbol{n}}\\ \underline{\boldsymbol{\Xi}} &= \left[\boldsymbol{\Xi}^{(0)}\mathrm{diag}\{\underline{\boldsymbol{s}}\}\underline{U},\ldots,\boldsymbol{\Xi}^{(P)}\mathrm{diag}\{\underline{\boldsymbol{s}}\}\underline{U}\right]\end{aligned} \tag{20}$$

where $\mathrm{diag}\{\cdot\}$ is a square diagonal matrix with entries given by its vector argument.

Our goal is the maximum-likelihood (ML) estimate of H given the observation model (20) and the statistical model (18). Such a ML estimate $\hat{H}$ may be conventionally obtained due to the minimizer

$$\begin{aligned}\hat{H} &= (\boldsymbol{I}_{P+1}\otimes\underline{U})\hat{\underline{H}}\\ \hat{\underline{H}} &= \arg\min_{\underline{H}}\left(N_o^{-1}\|\underline{\boldsymbol{y}} - \sqrt{E_s}\underline{\boldsymbol{\Xi}}\,\underline{H}\|^2 + \underline{H}^*(\boldsymbol{R}_c\otimes\boldsymbol{R}_f)^{-1}\underline{H}\right)\end{aligned} \tag{21}$$

where $\|\cdot\|$ is the Frobenius matrix norm. The above minimizer yields a closed-form solution

$$\begin{aligned}\hat{H} &= (\boldsymbol{I}_{P+1}\otimes\underline{U})\hat{\underline{H}}\\ \hat{\underline{H}} &= \frac{\sqrt{E_s}}{N_0}\left(\frac{E_s}{N_0}\underline{\boldsymbol{\Xi}}^*\underline{\boldsymbol{\Xi}} + \left(\boldsymbol{R}_c^{-1}\otimes\underline{\boldsymbol{R}}_f^{-1}\right)\right)^{-1}\underline{\boldsymbol{\Xi}}^*\underline{\boldsymbol{y}}.\end{aligned} \tag{22}$$

Note that the $\underline{N}(P+1)\times\underline{N}(P+1)$ matrix inverse in (22) may be precomputed if the estimation is done during the training phase, so that the reference signals $\underline{\boldsymbol{s}}$ are fixed. For practical sizes of P and $\underline{N}$, this matrix can be stored with a relatively small overhead, as compared with storing the received and/or processed data when N is big. The main computational effort is, therefore, owing the product $(\underline{\boldsymbol{\Xi}}^*\underline{\boldsymbol{y}})$ and further computation of $\hat{H}$ from $\hat{\underline{H}}$. It is easy to see that the total number of complex-valued multiplications is $2\underline{N}(P+1)N$. This number is comparable to $(\log_2 N+1)N$ multiplications required for the standard channel estimation. The bottleneck of (22) is, therefore, the online computation of $(\underline{\boldsymbol{\Xi}}^*\underline{\boldsymbol{y}})$ and a computation of $\underline{U}$ or its storage in case of offline computation. We next discuss how to further simplify the estimation procedure.

B. Simplified Estimator

In this section, we indicate how to simplify critical parts of the estimation procedure, namely, the computation of $(\underline{\boldsymbol{\Xi}}^*\underline{\boldsymbol{y}})$ and that of $\hat{H}$ from $\hat{\underline{H}}$. We also show how to compute an approximate inverse in (22), in order to avoid storing this matrix when necessary. One can check that

$$\underline{\boldsymbol{\Xi}}^*\underline{\boldsymbol{y}} = \underline{U}^*\mathrm{diag}\{\underline{\boldsymbol{s}}^*\}\left[\underline{\boldsymbol{\Xi}}^{(0)},\ldots,\underline{\boldsymbol{\Xi}}^{(P)}\right]^*\underline{\boldsymbol{y}}. \tag{23}$$

Next, we note that according to (8), matrices $\boldsymbol{\Xi}^{(p)}$ may be expressed as follows:

$$\begin{aligned}\boldsymbol{\Xi}^{(p)} &= \boldsymbol{F}^*\boldsymbol{D}^{(p)}\boldsymbol{F}\\ \boldsymbol{D}^{(p)} &= \mathrm{diag}\left\{\left(\frac{(k-\delta)}{N}\right)^p\right\}_{0\leq k\leq N}\end{aligned} \tag{24}$$

where $\boldsymbol{F}$ is the $N\times N$ unitary Fourier basis. Next, we use once again the asymptotic property of Toeplitz–Hermitian matrices [20]. According to this property, the eigenbasis of $\boldsymbol{R}_f$ tends asymptotically $N\to\infty$ to the Fourier basis. More precisely

$$\underline{U}\to\underline{\boldsymbol{F}}\quad\text{as}\quad N\to\infty,\quad \underline{\boldsymbol{F}} = \left[[\boldsymbol{F}^*]_1,\ldots,[\boldsymbol{F}^*]_{\underline{N}}\right]. \tag{25}$$

Finally, we note that $\underline{\boldsymbol{x}} = \boldsymbol{F}\underline{\boldsymbol{y}}$, being the IFFT of the received block in the frequency domain, is the received block in the time domain. Based on these observations, we obtain

$$\begin{aligned}\underline{\boldsymbol{\Xi}}^*\underline{\boldsymbol{y}} = \Bigg[&\left(\underline{\boldsymbol{F}}^*\mathrm{diag}\{\underline{\boldsymbol{s}}^*\}\boldsymbol{F}^*\boldsymbol{D}^{(0)}\underline{\boldsymbol{x}}\right)^T,\ldots\\ &\ldots,\left(\underline{\boldsymbol{F}}^*\mathrm{diag}\{\underline{\boldsymbol{s}}^*\}\boldsymbol{F}^*\boldsymbol{D}^{(P)}\underline{\boldsymbol{x}}\right)^T\Bigg]^T.\end{aligned} \tag{26}$$

The above matrix operation requires $(P+1)$ times N-point FFT, $(P+1)$ reduced IFFT of size $N\times\underline{N}(P+1)$, and $2(P+1)$ additional scalar multiplications per subcarrier whereas no storage is needed.

V. Linear Equalization and Leakage Removal

In this section, we consider a linear filter approach to handle the ICI introduced by a time-varying frequency-selective channel, described earlier in this paper. First of all, we recall the optimum MMSE solution. Next, we simplify the optimal solution, taking into account the properties of typical channels.

Our goal is to retrieve the vector of symbols $\boldsymbol{s}$ given the vector of received signal in the frequency domain, according to the data model (9). The standard MMSE solution is

$$\begin{aligned}\hat{\boldsymbol{s}} &= \sqrt{\frac{E_s}{N_0}}\boldsymbol{A}^*\left(\frac{E_s}{N_0}\boldsymbol{A}\boldsymbol{A}^* + \boldsymbol{I}_N\right)^{-1}\boldsymbol{y}\\ \boldsymbol{A} &= \sum_{p=1}^{P}\boldsymbol{\Xi}^{(p)}\mathrm{diag}\left\{\hat{H}^{(p)}\right\}.\end{aligned} \tag{27}$$

A direct implementation of (27) requires adaptive inversion of the $N\times N$ matrix, which depends on the empirical channel parameters $\hat{H} = [\hat{H}^{(0)^T},\ldots,\hat{H}^{(P)^T}]^T$. This operation is prohibitively complex for practical N. A simplification proposed in this paper is owing to the following observations.

Observation 1: The matrix $\boldsymbol{A}$ may be approximated by the band matrix $\underline{\boldsymbol{A}}$ with $(2Q+1)$ nonzero diagonals around the main diagonal that coincide with the corresponding diagonals of $\boldsymbol{A}$. The energy of the residual ICI caused by such an approximation is proportional to $(1/(1+Q))$.

Observation 2: Matrix $[(E_s/N_0)\boldsymbol{A}\boldsymbol{A}^* + \boldsymbol{I}_N]$ is positive definite, and its off-diagonal elements are vanishingly small when $(f_d/f_s)\ll 1$.

The first observation is based on the property of the diagonals of the Toeplitz–Hermitian matrices $\boldsymbol{\Xi}^{(p)}$ when N is big (see the Appendix). Based on this result, we adopt the approximation $\boldsymbol{A}\approx\underline{\boldsymbol{A}}$. The second observation is due to (16), showing that

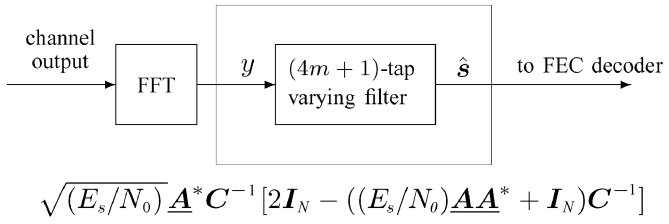

Fig. 1. Linear OFDM receiver with ICI removal.

the amplitude of $H^{(p)}$ decays as the pth power of (f_d/f_s) and the fact that only the derivatives $(p>0)$ contribute to the off-diagonal elements of $[(E_s/N_0)\boldsymbol{A}\boldsymbol{A}^*+\boldsymbol{I}_N]$. Later in this paper, we will see that practical values of (f_d/f_s) justify the first-order approximation of the matrix inverse in (27).

To make use of these approximations, we define an $N\times N$ diagonal matrix $\boldsymbol{C}$ which contains the main diagonal of $[(E_s/N_0)\boldsymbol{A}\boldsymbol{A}^*+\boldsymbol{I}_N]$. The simplified MMSE solution yields

$$\hat{\boldsymbol{s}}=\sqrt{\frac{E_s}{N_0}}\underline{\boldsymbol{A}}^*\boldsymbol{C}^{-1}\left(2\boldsymbol{I}_N-\left(\frac{E_s}{N_0}\underline{\boldsymbol{A}}\underline{\boldsymbol{A}}^*+\boldsymbol{I}_N\right)\boldsymbol{C}^{-1}\right)\boldsymbol{y}. \quad (28)$$

Since $\boldsymbol{C}$ is diagonal, computing $\boldsymbol{C}^{-1}$ yields N divisions. In terms of complexity, computing $\boldsymbol{C}^{-1}$ and its product with an $N\times 1$ vector substitutes the standard equalization (i.e., computing $\boldsymbol{C}^{-1}$ and its product with $\boldsymbol{y}$) in the conventional OFDM. Note also that $\underline{\boldsymbol{A}}$ and $[((E_s/N_0)\underline{\boldsymbol{A}}\,\underline{\boldsymbol{A}}^*+\boldsymbol{I}_N)\boldsymbol{C}^{-1}]$ are band matrices with $(2Q+1)$ and $(4Q+1)$ nonzero diagonals correspondingly. Therefore, the additional complexity of (28) is approximately $[(4Q+1)N+(2Q+1)N+2N]$, that is, $(6Q+4)$ complex-valued operations per subcarrier, compared with the conventional OFDM demodulation.

A block diagram of the proposed ICI-resilient OFDM receiver is plotted in Fig. 1. The difference w.r.t. the conventional OFDM receiver lies in an additional filtering stage, prior to the slicing or soft-output computation, depending on forward error correction (FEC) decoder to be used. The finite impulse response (FIR) filter has $(4Q+1)$ taps and varies depending on the subcarrier. According to (28), the tap coefficients corresponding to the kth subcarrier are given by $(4Q+1)$ nonzero entries of the kth row of the filter matrix, which is a band matrix with $(4Q+1)$ nonzero diagonals. It is worthwhile to recall a linear filtering approach to ICI removal presented in [18]. The authors suggested making use of a simplified zero-forcing (ZF) filter in order to remove the first-order approximation of ICI (similar to $p=0$ in our case). A simplified ZF solution is computed due to a band approximation of the ICI contribution on one hand, and replacing of the $N\times N$ matrix inverse by around N inverses of *local* matrices within a certain window in the frequency domain. The minimum window size equals three, which in terms of the $(2Q+1)$-band approximation yields $Q=1$. Further increase of the window size makes the implementation impossible, since it implies a complexity of $O((2Q+1)^3)$ per subcarrier. In [21], we showed that choosing Q too small leads to a significant performance degradation. The approach described here allows achieving a reasonable complexity.

VI. Decision-Feedback Receiver

A numerically efficient DFE for the frequency-domain equalization and ICI removal can be built, taking into account the structure of the leakage matrices $\boldsymbol{\Xi}^{(p)}$, $p>0$. The core idea of the present DFE solution is to exploit the results of the standard OFDM demodulation in order to remove the ICI interference, and subsequently perform a new detection over the (almost) ICI-free data. Denote $\tilde{\boldsymbol{s}}=[\tilde{\boldsymbol{s}}_0,\ldots,\tilde{\boldsymbol{s}}_{N-1}]^T$ a vector of decisions obtained by slicing or FEC decoding applied to the output $E_s^{-1/2}\boldsymbol{B}^{-1}\boldsymbol{y}$ of the OFDM equalizer that ignores the ICI; here, $\boldsymbol{B}$ is a $N\times N$ diagonal matrix built of the respective diagonal elements of $\boldsymbol{A}$. Then, the ICI-free data may be obtained as follows:

$$\hat{\boldsymbol{s}}=\boldsymbol{B}^{-1}\left(\frac{\boldsymbol{y}}{\sqrt{E_s}}-\left(\sum_{p=1}^{P}\left(\boldsymbol{\Xi}^{(p)}-\Gamma_p\boldsymbol{I}_N\right)\mathrm{diag}\left\{\hat{H}^{(p)}\right\}\right)\tilde{\boldsymbol{s}}\right)$$

$$\Gamma_p=\frac{1}{N}\sum_{j=1}^{N}\left(\frac{(j-\delta)}{N}\right)^p.$$

Here, Γ_p stand for diagonal entries of $\boldsymbol{\Xi}^{(p)}$, $1\le p\le P$. Note that the direct implementation of such a DFE requires multiplication of an $N\times 1$ vector by an $N\times N$ matrix which is prohibitively complex for big N. To reduce the complexity, we use the result (24) for $\boldsymbol{\Xi}^{(p)}$, $1\le p\le P$. Check that

$$\hat{\boldsymbol{s}}=\boldsymbol{B}^{-1}\left(\frac{\boldsymbol{y}}{\sqrt{E_s}}-\boldsymbol{F}^*\sum_{p=1}^{P}\tilde{\boldsymbol{D}}^{(p)}\boldsymbol{F}\mathrm{diag}\left\{\hat{H}^{(p)}\right\}\tilde{\boldsymbol{s}}\right)$$

$$\tilde{\boldsymbol{D}}^{(p)}=\mathrm{diag}\left\{\left(\frac{(k-\delta)}{N}\right)^p-\Gamma_p\right\}_{0\le k<N}. \quad (29)$$

A block diagram of the DFE receiver constructed according to (29) is given in Fig. 2. As it follows from this block diagram, the additional cost of the simplified DFE solution compared with the standard OFDM demodulation consists of $(P+1)$ N-point FFT and $(2P+1)$ extra multiplications per subcarrier.

VII. Channel Extrapolation

As explained in Section IV, the estimation of channel parameters is based on training block or a previous data block which is assumed successfully demodulated. In both cases, a channel estimate obtained for a current block is used to process the following block. In the presence of fast channel variations, such an estimate will no longer be accurate. Hence, one needs to predict the channel parameters that are valid for the upcoming data block.

Since the set of amplitudes and derivatives characterizes static as well as dynamic properties of the channel, they may be used to track channel variations. Recall that (10) stands for the time-varying frequency response at the kth subcarrier at time instance $(j-\delta)T$. Herein $\tilde{H}_l[k]$ stands for the complex contribution of the lth propagation path at a reference time, while the term $(\imath 2\pi f_l(j-\delta)T)$ extrapolates the phase of this path at $(j-\delta)T$. Finally, the sum over all paths results in a total time-varying

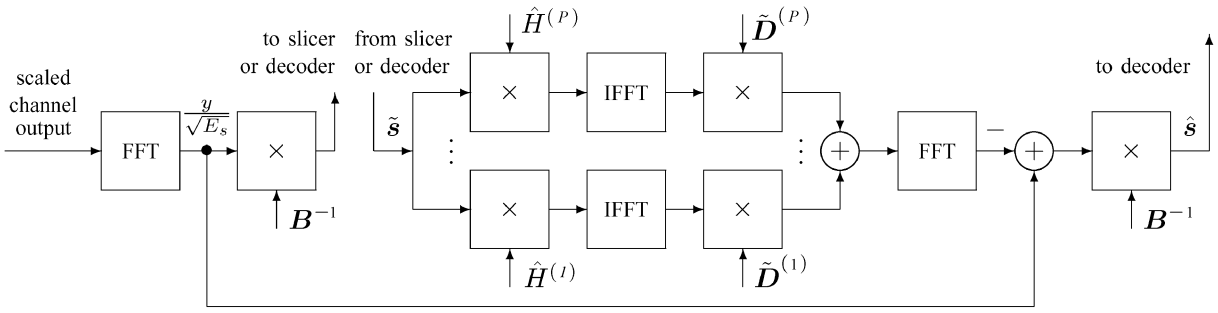

Fig. 2. DFE-OFDM receiver with ICI removal.

frequency response. According to the definition (7) of derivatives, we may write a power series expansion of the frequency response w.r.t. time, as follows:

$$\begin{aligned}\sum_l \tilde{H}_l[k]e^{\imath 2\pi f_l(j-\delta)T} &= \sum_{l,p} \tilde{H}_l[k]\frac{(\imath 2\pi f_l)^p}{p!}((j-\delta)T)^p \\ &= \sum_p ((j-\delta)f_sT)^p \frac{\left(\frac{\imath 2\pi f_d}{f_s}\right)^p}{p!} \\ &\quad \times \sum_l \tilde{H}_l[k]\left(\frac{f_l}{f_d}\right)^p \\ &= \sum_p \left(\frac{(j-\delta)}{N}\right)^p H_k^{(p)}. \end{aligned} \tag{30}$$

The right-hand side (RHS) of (30) specifies a polynomial extrapolation of the time-varying frequency response over a time interval $(j-\delta)T$. As we need to extrapolate the channel response over one data block duration (including cyclic extension), we have $(j-\delta)=(N+L)$. Further use of (30) yields the following update of amplitudes and derivatives:

$$\hat{H}^{(p)} := \sum_{q\geq p}\left(1+\frac{L}{N}\right)^{q-p}\hat{H}^{(q)}, \quad 0\leq p<P. \tag{31}$$

The latter expression implies that extrapolating amplitudes and P derivatives requires at least $(P+1)$ estimated derivatives. For Doppler rates of practical relevance, the power contained in higher order derivatives decreases fast along with the order, see (16). This fact allows us to neglect temporal variations of higher order derivatives.

VIII. Residual ICI

Based on the statistical characterization of the time-varying channel from the previous section, we can compute the relative level of the residual (nonremoved) ICI. The residual interference defines an effective noise floor, which limits system performance as well as the attainable spectral efficiency.

To compute the level of such a noise floor after partial ICI removal, we assume that the channel estimation and ICI removal take into account the derivatives of orders $1,\ldots,P$. It is easy to see that the residual interference is defined by the terms of the sum in (9) with $p>P$. Define $\mathcal{I}_P$ as the average ICI energy per subcarrier. According to (8) and under the standard assumption of i.i.d. data symbols $\boldsymbol{s}_k$, we can express the average energy of ICI per subcarrier as follows:

$$\begin{aligned}\mathcal{I}_P &= \frac{E_s}{N}\sum_{k,m=0}^{N-1}\sum_{p,q>P}\mathbb{E}\left\{H_k^{(p)}H_k^{(q)^*}\right\}\Xi_{m,k}^{(p)}\Xi_{m,k}^{(q)^*} \\ &= E_s\sum_{p,q>P}[\boldsymbol{R}_c]_{p,q}\frac{1}{N}\sum_{j=0}^{N-1}\left(\frac{(j-\delta)}{N}\right)^{p+q}\end{aligned}$$

where the RHS is due to $\mathbb{E}\{H_k^{(p)}H_k^{q^*}\} = [\boldsymbol{R}_c]_{p,q}$ [see (14)–(16)] and due to (24). The latter expression may be further simplified by acknowledging that for $\delta=(N-1)/2$

$$\frac{1}{N}\sum_{j=0}^{N-1}\left(\frac{(j-\delta)}{N}\right)^{p+q} \to \int_{-\frac{1}{2}}^{+\frac{1}{2}} v^{p+q}dv = \frac{2^{-(p+q)}}{p+q+1}$$

as $N\to\infty$ for even $(p+q)$ and is null for odd $(p+q)$. The last two expressions and (16) yield, after a straighforward calculus, the following large sample $(N\to\infty)$ expression for $\mathcal{I}_P$:

$$\mathcal{I}_P = E_s\sum_{k=P+1}^{\infty}\frac{1-2^{-2k}\sum_{p=0}^{P}\binom{2k}{p}}{(k!)^2(2k+1)}\left(\frac{\pi f_d}{f_s}\right)^{2k}.$$

Finally, the signal-to-noise-and-interference ratio (SINR) $\gamma_P^2 \triangleq E_s/(N_0+\mathcal{I}_P)$ is given by

$$\gamma_P^2 = \frac{1}{\left(\frac{E_s}{N_0}\right)^{-1}+\sum_{k=P+1}^{\infty}\frac{1-2^{-2k}\sum_{p=0}^{P}\binom{2k}{p}}{(k!)^2(2k+1)}\left(\frac{\pi f_d}{f_s}\right)^{2k}}. \tag{32}$$

Note that the infinite series in (32) have superexponential convergence w.r.t. P. Hence, only a few terms of this series should be taken into account.

IX. Numerical Study

In this paper, we consider the DVB application with the European DVB-T standard being considered as the reference. This standard specifies the use of either 2-K mode (2048 subcarriers) or 8-K mode (8192 subcarriers) with the signal bandwidth of 8 MHz in both cases. The 8-K mode allows one to keep a cyclic extension short, compared with the total OFDM block size, thereby increasing the spectral efficiency. In fact, 8 K appears to be preferred mode for stationary (low-mobility) scenarios. A high-rate transmission is enabled within the standard, due to the 64-QAM signaling with FEC code rates ranging from

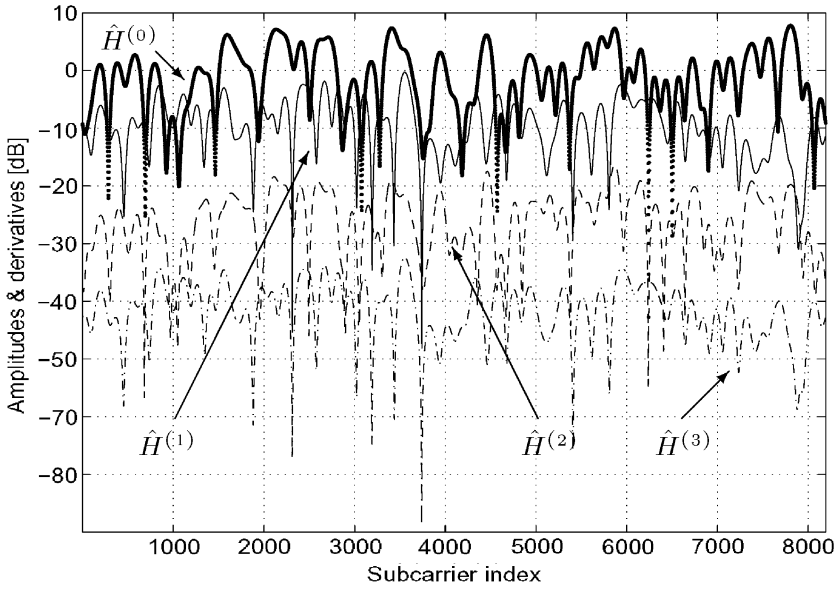

Fig. 3. Empirical amplitudes/derivatives $\hat{H}^{(p)}$ dB versus subcarrier index.

1/2 to 7/8. These rates are achieved by puncturing the standard 64-state rate-1/2 convolutional code with the generating polynomial (171_8, 133_8). Such an inner code is meant to provide the error rate no more than $2 \cdot 10^{-4}$ in order to ensure the quasi-error-free operation due to the outer Reed–Solomon code. In the present simulation setup, we will consider carrier frequency 640 MHz, 8-K mode with 1/32 cyclic extension overhead (i.e., $L/N = 1/32$) and code rate 2/3, all resulting in the data rate 24.13 Mb/s.

A. Channel Modeling

We will assume frequency-selective channels with the rms delay spread $\tau_0 = 4$ μs. The propagation channel is a superposition of a large number of scatterers with random delays $\{\tau_l\}$. The contributions $\{h_l\}$ of these scatterers are generated as independent zero-mean complex Gaussian variables with variances that follow the delay profile as defined in (1). The respective directions of arrival $\{\theta_l\}$ are i.i.d. uniformly distributed within $(-\pi, \pi)$. Whenever a mobile environment is considered, we will assume a downlink scenario with the terminal velocity 120 km/h. According to DVB-T specifications, baseband signal is subject to a zero-rolloff pulse shaping. At the receiver, the filtered signal is subject to timing recovery and sampling at the baud rate $(1/T)$.

In Fig. 3, one can see empirical channel parameters, namely, amplitudes $\hat{H}^{(0)}$ and derivatives $\hat{H}^{(1)}$ through $\hat{H}^{(3)}$ obtained from a mobile channel realization with the settings as described above, and (E_s/N_0) of 30 dB. The parameters are estimated according to the ML procedure described in Section IV with $\underline{N} = 60$. Note that derivatives $\hat{H}^{(3)}$ have a negligible contribution to the received signal. Admittedly, the estimation accuracy of $\hat{H}^{(3)}$ is low, relative to their power level. Meanwhile, $\hat{H}^{(1)}$ contributes substantially, resulting in a substantial ICI level. This ICI level limits the overall noise floor, and thereby disables the required QoS for the spectral efficiency under consideration, which requires (E_s/N_0) around 20 dB and higher, depending on channel statistics [22]. To highlight the necessity of ICI removal in this example, we applied the conventional demodulation and equalization procedure with no ICI removal. Precisely, the set $\hat{H}^{(0)}, \ldots, \hat{H}^{(3)}$ has been used to extrapolate $\hat{H}^{(0)}$, as explained in Section VII. The empirical channel response $\hat{H}^{(0)}$ was exploited for the standard demodulation, equalization, and decoding. The percentage of erroneously coded bits (hard decisions after soft demapping) and user bits (after Viterbi decoding) in this example was 5.4% and 0.5%, respectively.

B. Terminal Velocity and SINR

To analyze the effect of terminal velocity on the receiver performance with and without ICI cancellation, we make use of (32) for the residual SINR. Note that $P = 0$ corresponds to the SINR at the output of the conventional OFDM demodulator, while $P > 0$ represents the SINR achievable with a perfect estimation and removal of ICI, which is approximated by amplitudes and derivatives up to the Pth order. Note that γ_P^2 stands for the upper bound on the SINR, which assumes perfect ICI removal.

The top panel of Fig. 4 shows the SINR γ_P^2 versus the input SNR (E_s/N_0) for $P = 0, 1, 2$ and terminal velocity 120 km/h. Note that the SINR is limited by 18 dB for the conventional receiver $(P = 0)$ achievable at the input SNR of 30 dB. Reaching the 20-dB level of SINR required for successful reception in the considered transmission mode (24.13 Mb/s) is practically impossible without ICI cancellation. Conversely, ICI cancellation with the first-order approximation $(P = 1)$ removes the noise floor caused by ICI. Note that higher order approximations (here $P = 2$) give no visible improvement.

The bottom panel of Fig. 4 displays SINR versus terminal velocity for $E_s/N_0 = 30$ dB and $P = 0, 1, 2$. Note that SINR degrades dramatically along with the velocity increase in the absence of ICI cancellation. For speeds approaching 300 km/h (high-speed trains in Europe and Japan), the SINR drops below the level of 11–12 dB, thereby disabling even lower spectral effi-

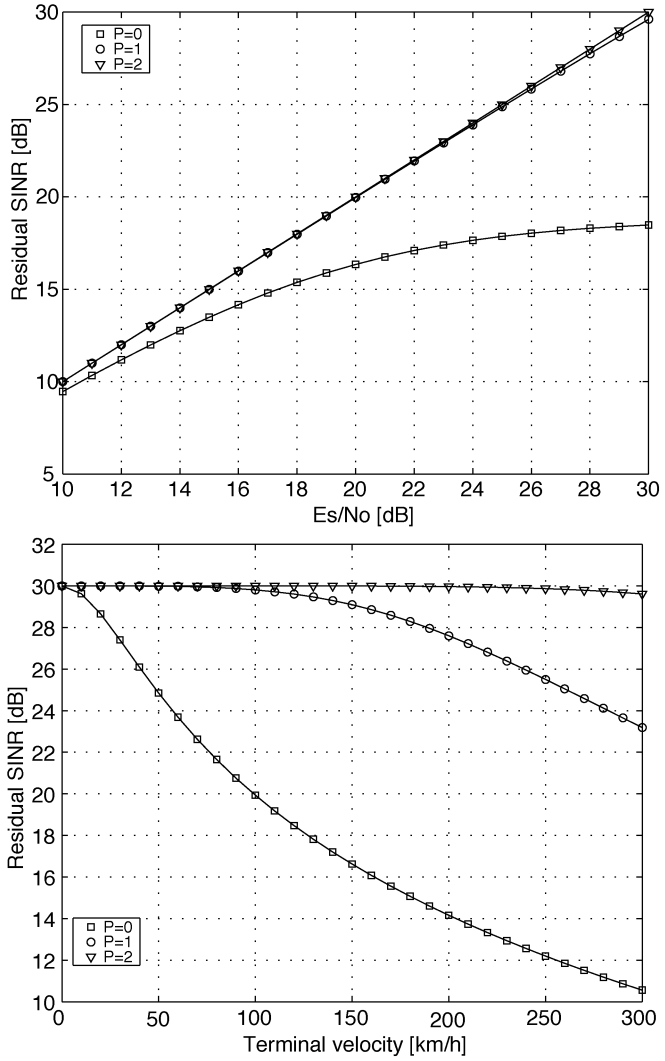

Fig. 4. Theoretically achievable SINR for different orders P versus (E_s/N_o) dB, velocity 120 km/h (top) and versus velocity (km/h), $E_s/N_o = 30$ dB (bottom).

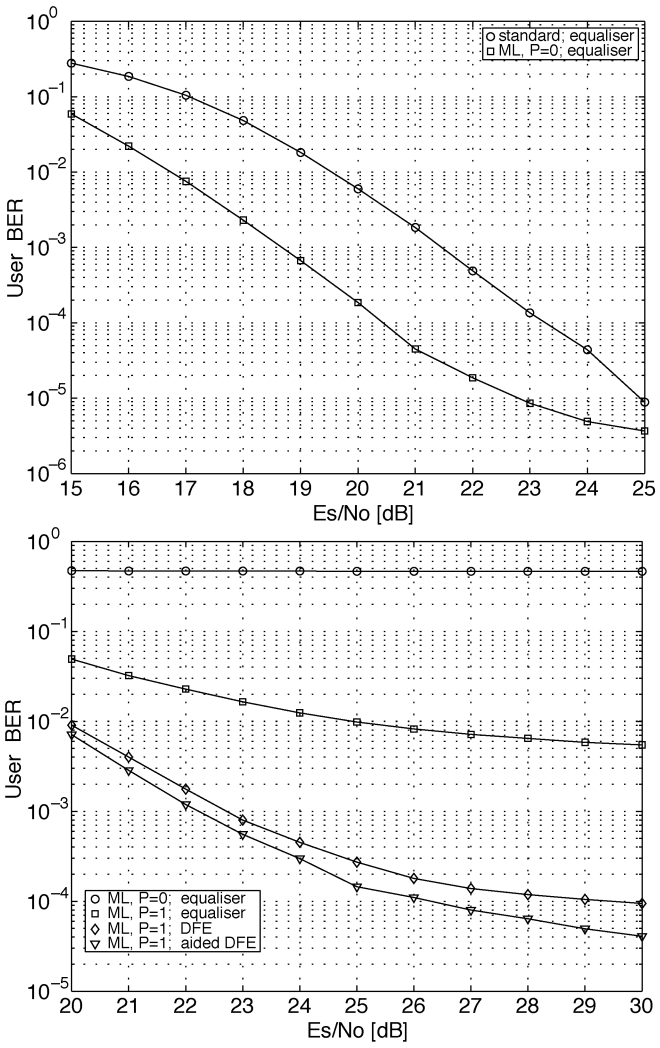

Fig. 5. User BER versus (E_s/N_0) dB for various estimators and ICI cancellers; static channel (top) and velocity 120 km/h, $P = 1$ (bottom).

ciencies (corresponding 16-QAM signaling in DVB-T). Meanwhile, low-order ICI cancellation ($P = 1, 2$) would provide ICI immunity for the practical velocities.

C. Bit-Error Rates

We now consider the user bit-error rate (BER) (after Viterbi decoding) of the DVB-T receiver with the settings described at the beginning of Section IX. First, we assume a static environment (no mobility). In the top panel of Fig. 5, we plot BER versus the input SNR for two different channel estimators. Here, $(-\circ-)$ shows BER obtained with no channel statistics involved. This scheme assumes independent channel response within each frequency bin. The ML procedure described in Section IV, with $P = 0$ and $\underline{N} = 60$, results in BER plotted by $(-\square-)$. Both estimators are based on a single training OFDM block. Upon static channel estimation, the conventional equalization and decoding apply. The gain in performance is due to the use of channel statistics which, due to a decaying delay profile, yields a reduced number of effective parameters. In essence, this observation is reminiscent of the results in [11]. Note that with accurate channel estimation, the SNR of 20 dB is needed to meet the QoS requirements.

The bottom panel of Fig. 5 shows BER achieved with different channel estimation and ICI removal procedures for the mobile velocity of 120 km/h. The result of ML static channel estimation $(P = 0)$ and the conventional equalization/decoding is plotted here by $(-\circ-)$. The curve $(-\square-)$ shows BER obtained due to ML estimation of ICI channel $(P = 1)$, with the subsequent channel interpolation as indicated in Section VII and the conventional equalization and decoding steps. A noticeable improvement in BER as opposed to the previous curve is owing to the channel interpolation, which is based on the estimated dynamic component of the ICI channel. However, the impact of ICI is not removed, so that the minimum level of BER remains far above the QoS requirements $(2 \cdot 10^{-4})$. The results of ICI cancellation based on the ML estimation $(P = 1)$, channel interpolation, and the ICI-resilient DFE described in Section VI are plotted by $(-\diamond-)$. One can see an improved BER achieving the QoS requirements at the input SNR of around 26 dB. Finally, $(-\triangledown-)$ shows the performance of a *genie-aided* DFE, wherein the intermediate decisions $\tilde{\boldsymbol{s}}$ are replaced by the correct symbols.

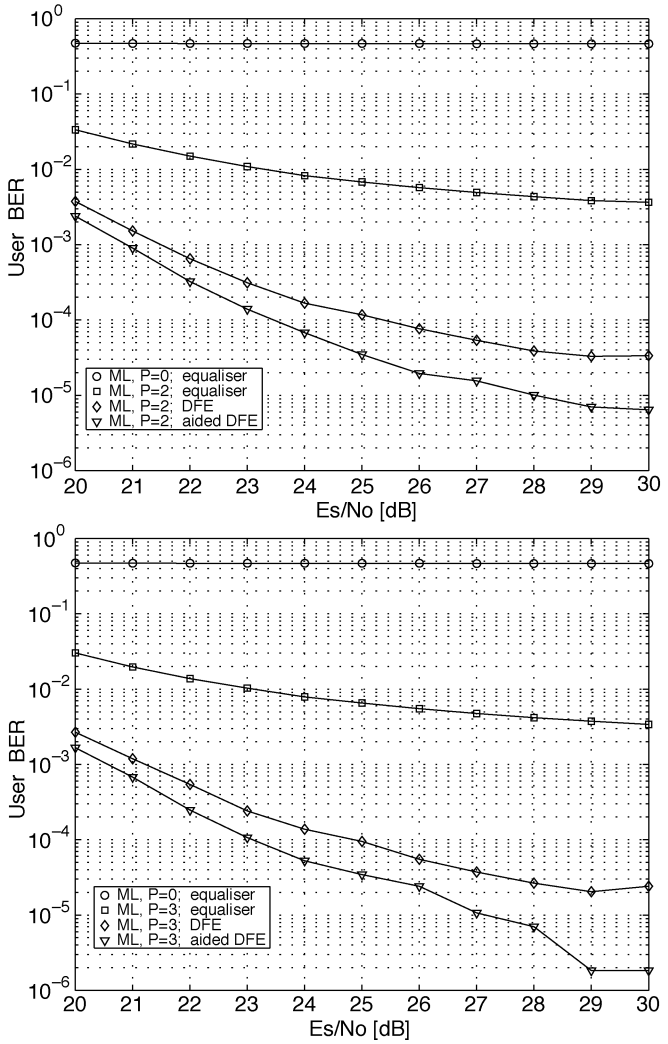

Fig. 6. User BER versus (E_s/N_0) dB for various estimators and ICI cancellers, velocity 120 km/h; $P = 2$ (top) and $P = 3$ (bottom).

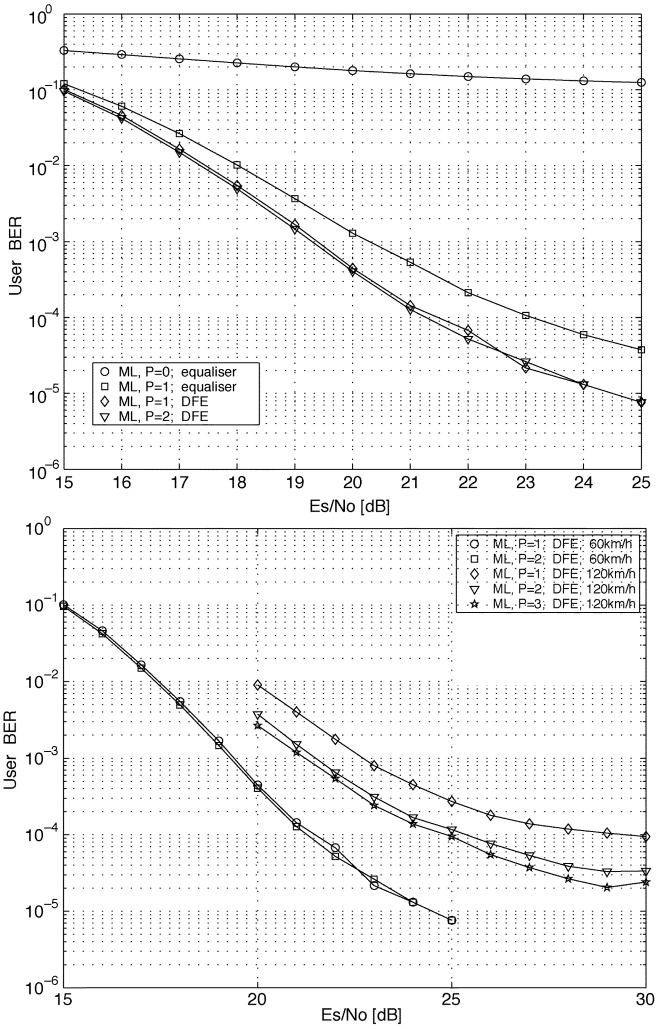

Fig. 7. User BER versus (E_s/N_0) dB for various estimators and ICI cancellers, velocity 60 km/h; (top) and various orders P, velocities 60 km/h and 120 km/h (bottom).

This result shows a penalty of 1.5 dB caused by error propagation within the DFE.

In Fig. 6, we show BER achieved by the same receiver architectures for higher orders, $P = 2$ in the top panel and $P = 3$ in the bottom panel. The increased approximation order P allows reducing the required input SNR by 2 dB $(P = 2)$ and 2.7 dB $(P = 3)$. Further increase of the order P is not beneficial in this scenario. When compared with the standard DVB-T receiver with ML channel estimation and low-mobility environment, the proposed ICI-resilient DFE yields the required BER at a cost of an additional 3.3 dB.

In the top panel of Fig. 7, we compare the same receiver architectures for the terminal velocity 60 km/h. Note that ignoring the mobile nature of the channel $(P = 0)$ leads to a dramatic performance degradation. The required QoS may be reached at the SNR of 22 dB when the first-order approximaton is used to track the channel. Further ISI removal reduces this level by about 1.3 dB. However, the benefit of a higher approximation order $(P = 2)$ is marginal. Finally, BER results for DFE-based ICI cancellation with different approximation orders are summarized in the bottom panel of Fig. 7. Let us emphasize that the increase of the order from $P = 1$ to $P = 2$ leads to a gain of 2 dB for 120 km/h, despite the fact that the theoretical residual ICI level is almost the same in both cases, see Fig. 4. The improvement is mainly due to an incresed channel tracking accuracy, that is, a higher quality of channel extrapolation (see Section VII), rather than a more accurate ICI removal within an OFDM block.

X. Summary and Discussions

In this paper, we introduced a general framework to quantify and control the impact of the ICI on the performance of mobile OFDM systems. A compact model of the ICI channel is owing to a finite power series expansion of a time-varying channel w.r.t. to Doppler shifts of individual propagation paths. Such a representation gives rise to a scalable parameterization of ICI channels. The number of parameters can be adapted according to the desired tradeoff between the accuracy and the complexity. Statistical characterization of time and Doppler spread based on the Jakes model were used to design an ML estimator of ICI channel parameters. In Section IV-B, we made use of the structural properties of the ML estimator to build a reduced-complexity estimate. We considered two different approaches to ICI removal.

The first one is a linear MMSE receiver, whereas the second one has decision-feedback architecture. For both receivers, we made use of the structure of ICI channels to achieve reduced-complexity implementations.

In this paper, we addressed mobile reception of DVB-T. Robust reception for mobile DVB-T represents a major challenge, primarily because of big delay and Doppler spreads, along with a request for high spectral efficiencies, and a big OFDM block size (8192 subcarriers in 8-K mode) which imposes severe complexity constraints. As we demonstrated in the previous section, a reduced-complexity ML channel estimation and subsequent ICI removal by means of DFE enables high spectral efficiencies, along with high mobility under the standard QoS requirements. Other receivers, such as the linear MMSE receiver presented in Section V and other competing schemes (see, e.g., [18]), are not applicable in DVB-T because of excessive complexity. A numerical study of MMSE receivers has been recently presented in [21].

It is worth mentioning that channel tracking remains an important issue for mobile OFDM. Our numerical experience suggests that channel extrapolation, described in Section VII, is more sensitive to the choice of model order P than the subsequent ICI removal. This fact motivates frequent updates of channel estimates, based, e.g., on previously decoded blocks, thereby increasing the overall complexity. Finding a suitable balance of performance and complexity in the 8-K mode of DVB-T is the central focus of our present efforts.

APPENDIX

Deterministic Timing

As explained in Section III, the timing t_0 is chosen which maximizes the received power

$$\hat{t}_0 = \arg\max_{t_0} \mathbb{E}\left\{||\boldsymbol{y}||^2\right\} \tag{33}$$

where the expectation is w.r.t. $\boldsymbol{s}$ only. To find $\mathbb{E}\{||\boldsymbol{y}||^2\}$, we use (5), (6), and the fact that the entries of $\boldsymbol{s}$ are zero mean and unit variance i.i.d. After summing w.r.t. m, we obtain

$$\begin{aligned}\mathbb{E}\left\{||\boldsymbol{y}||^2\right\} &= \sum_{m=0}^{N-1} |\boldsymbol{y}_m|^2 \\ &= \frac{E_s}{N^2}\sum_{k=0}^{N-1}\sum_{j=0}^{N-1}\sum_{l,l'} \tilde{H}_l[k]\tilde{H}_{l'}[k] e^{\imath 2\pi (f_l - f_{l'})T(j-\delta)} \\ &= \frac{E_s}{N^2}\sum_{k=0}^{N-1}\sum_{j=0}^{N-1}\sum_{l,l'}\sum_{i,i'} h_l h_{l'}^* e^{\imath 2\pi (f_l - f_{l'})(t_0+T_j)} \\ &\quad \cdot g(t_0-\tau_l+iT)g(t_0-\tau_{l'}+i'T)e^{\frac{-\imath 2\pi k(i-i')}{N}}.\end{aligned}$$

By the law of big numbers, **As1** yields

$$\sum_{\substack{\tau_l\in(\tau,\tau+d\tau)\\ \tau_{l'}\in(\tau',\tau'+d\tau)}} h_l h_{l'}^*, e^{\imath 2\pi (f_l - f_{l'})(t_0+T_j)} = \delta_{\tau,\tau'} \sum_{\tau_l\in(\tau,\tau+d\tau)} |h_l|^2$$

with probability one for any τ, τ', $d\tau > 0$. Due to this result and continuity of $g(\cdot)$, we may write

$$\begin{aligned}\mathbb{E}\left\{||\boldsymbol{y}||^2\right\} &= \frac{E_s}{N^2}\sum_{k,j=0}^{N-1}\sum_{l}|h_l|^2\left|\sum_i g(t_0-\tau_l+iT)e^{-\imath\frac{2\pi ki}{N}}\right|^2 \\ &= E_s|h_l|^2\left|\sum_i g(t_0-\tau_l+iT)e^{-\imath\frac{2\pi ki}{N}}\right|^2.\end{aligned}$$

According to (1), the last expression equals

$$\mathbb{E}\left\{||\boldsymbol{y}||^2\right\} = \frac{E_s}{\tau_0}\int_0^\infty e^{-\frac{\tau}{\tau_0}}\left|\sum_i g(t_0-\tau+iT)e^{-\imath\frac{2\pi ki}{N}}\right|^2 d\tau$$

with probability one, and therefore, $\hat{t}_0$ in (33) is a deterministic quantity (independent on channel realization) which is defined in Section III.

Observation 1: Let us make use of the following recursion ($N\to\infty$):

$$\begin{aligned}\Xi_{k,k+m}^{(0)} &= \delta_{k,k+m} \\ \Xi_{k,k+m}^{(p)} &= \frac{1}{N}\sum_{j=0}^{N-1}\left(\frac{j-\delta}{N}\right)^p e^{\imath 2\pi\frac{m(j-\delta)}{N}} \\ &\to \int_{-\frac{1}{2}}^{\frac{1}{2}} v^p e^{\imath 2\pi m v}dv \\ &= \frac{1}{\imath 2\pi m}\left(\alpha - p\int_{-\frac{1}{2}}^{\frac{1}{2}} v^{p-1}e^{\imath 2\pi m v}dv\right) \\ &\to \frac{1}{\imath 2\pi m}\left(\alpha - p\Xi_{k,k+m}^{(p-1)}\right), \quad p>0\end{aligned}$$

where $\alpha = (-1)^m 2^{-(p+1)}(1-(-1)^{p+1})$. According to this result, $\sup_p |\Xi_{k,k+m}^{(p)}| = O(1/m)$. By the definition of $\boldsymbol{A}$, the residual ICI energy satisfies

$$\sum_{|m|>1+Q}\mathbb{E}\left\{|\boldsymbol{A}_{k,k+m}|^2\right\} = \sum_{|m|>1+Q} O\left(\frac{1}{m^2}\right) = O\left(\frac{1}{1+Q}\right).$$

REFERENCES

[1] R. W. Chang, "Synthesis of bandlimited orthogonal signals for multichannel data transmission," *Bell Syst. Tech. J.*, vol. 45, pp. 1775–1796, Dec. 1966.

[2] S. B. Weinstein and P. M. Ebert, "Data transmission by frequency-division multiplexing using the discrete Fourier transform," *IEEE Trans. Commun.*, vol. COM-19, pp. 628–634, Oct. 1971.

[3] B. Hirosaki, "An orthogonally multiplexed QAM system using discrete Fourier transform," *IEEE Trans. Commun.*, vol. COM-29, pp. 982–989, July 1981.

[4] L. Cimini, Jr., "Analysis and simulation of a digital mobile channel using orthogonal frequency-division multiplexing," *IEEE Trans. Commun.*, vol. COM-33, pp. 665–675, July 1985.

[5] J.-P. Linnartz and S. Hara, "Editorial introduction for special issue on multicarrier communications," *Wireless Pers. Commun.*, vol. 2, no. 1, pp. 1–7, 1995.

[6] B. Le Foch, M. Alard, and C. Berrou, "Coded orthogonal frequency-division multiplex," *Proc. IEEE*, vol. 83, pp. 982–995, June 1995.

[7] N. Y. Lee, J.-P. Linnartz, and G. Fettweis, "Multicarrier CDMA in indoor wireless radio networks," in *Proc. PIMRC*, 1993, pp. 109–113.

[8] K. Fazel and P. Papke, "On the performance of convolutionally coded CDMA/OFDM for mobile communication system," in *Proc. PIMRC*, 1993, pp. 468–472.
[9] M. Russell and G. Stüber, "Interchannel interference analysis of OFDM in a mobile environment," in *Proc. Vehicular Technology Conf.*, 1995, pp. 820–824.
[10] P. Robertson and S. Kaiser, "The effects of Doppler spreads in OFDM(A) mobile radio systems," in *Proc. Vehicular Technology Conf.—Fall*, 1999, pp. 329–333.
[11] Y. Li, L. J. Cimini, and N. R. Sollenberger, "Robust channel estimation for OFDM systems with rapid dispersive fading channels," *IEEE Trans. Commun.*, vol. 46, pp. 902–915, July 1998.
[12] C. Jakes, *Microwave Mobile Communications*. New York: Wiley, 1974.
[13] T. Aulin, "A modified model for the fading signal at a mobile radio channel," *IEEE Trans. Veh. Technol.*, vol. VT-28, pp. 182–203, Mar. 1979.
[14] E. Jaffrot and M. Siala, "Turbo channel estimation for OFDM systems on highly time and frequency selective channels," in *Proc. ICASSP*, vol. 5, June 2000, pp. 2977–2980.
[15] J. Armstrong, P. Grant, and G. Porey, "Polynomial cancellation coding of OFDM to reduce intercarrier interference due to Doppler spread," in *Proc. GLOBECOM*, 1998, pp. 2771–2776.
[16] Y. Zhao and S.-G. Häggmam, "Intercarrier interference self-cancellation scheme for OFDM mobile communication systems," *IEEE Trans. Commun.*, vol. 49, pp. 1185–1191, July 2001.
[17] G. Gueslin, "Equalization of FFT-leakage in mobile DVB-T," Master's thesis, Roy. Inst. Technol., Stockholm, Sweden, 1998.
[18] W. G. Jeon, K. H. Chang, and Y. S. Cho, "An equalization technique for OFDM systems in time-variant multipath channels," *IEEE Trans. Commun.*, vol. 47, pp. 27–32, Jan. 1999.
[19] R. H. Clarke, "A statistical theory of mobile radio reception," *Bell Syst. Tech. J.*, vol. 47, pp. 987–1000, 1968.
[20] R. Gray, "On the asymptotic eigenvalues of Toeplitz matrices," *IEEE Trans. Inform. Theory*, vol. IT-18, pp. 725–730, May 1972.
[21] J.-P. Linnartz and A. Gorokhov, "New equalization approach for OFDM over dispersive and rapidly time-varying channel," in *Proc. PIMRC*, Sept. 2000, pp. 1375–1379.
[22] *Digital Video Broadcasting (DVB); Framing Structure, Channel Coding and Modulation for Digital Terrestrial Television*, Eur. Standard EN 300 744 v1.2.1 ed., 1999.

Alexei Gorokhov (S'96–A'97) received the Ph.D. degree in electrical engineering in 1997 from École Nationale Supérieure des Télécommunications (Télécom Paris), Paris, France.

From October 1997 to January 2000, he was a Scientist with the Centre National de la Recherche Scientifique (CNRS) in France. From January 2000 to November 2003, he was with Philips Research Labs, Eindhoven, The Netherlands. In November 2003, he joined Qualcomm Inc., San Diego, CA. His research interests cover various areas of digital communications, estimation theory and spectral analysis, with particular emphasis on the analysis and design of multiantenna (MIMO) systems and multicarrier communication systems.

Jean-Paul Linnartz (S'85–M'87–SM'99) received the Ph.D. degree in 1991 from Delft University of Technology, Delft, The Netherlands.

He is currently a Department Head with the Natuurkundig Laboratorium (Nat. Lab.) of Philips Research, Eindhoven, The Netherlands. His team actively participates in various standardization forums for content protection, digital rights management, and wireless communication. Earlier, as a Principal Scientist, he studied the protection of audio and video content, in particular using the technology of electronic watermarking. In 1992–1993, he was an Assistant Professor at The University of California at Berkeley, where he worked on random access to wireless networks. In 1993, he was the first to use the name multicarrier CDMA, in one of the pioneering papers on the combination of OFDM with CDMA. He has 20 (pending) patents in the field of electronic watermarking, copy protection, and radio communications. He has authored over 100 papers, is founding Editor-in-Chief of *Wireless Communication, The Interactive Multimedia CD-ROM*, and he has been Guest Editor for two special journal issues on OFDM and multicarrier modulation.